

Article

A Multi-Analytical Study of an Ancient Egyptian Limestone Stele for Knowledge and Conservation Purposes: Recovering Hieroglyphs and Figurative Details by Image Analysis

Tiziana Cavaleri ^{1,2} , Stefano Legnaioli ^{3,*} , Francesca Lozar ⁴, Cesare Comina ⁴, Federico Poole ⁵,
Claudia Pelosi ² , Alessia Spoladore ⁶, Daniele Castelli ⁴ and Vincenzo Palleschi ³ 

- ¹ Centro Conservazione e Restauro dei Beni Culturali La Venaria Reale, Venaria Reale, 10078 Turin, Italy; tiziana.cavaleri@centrorestaurovenaria.it or tiziana.cavaleri@unitus.it
- ² Dipartimento di Economia, Ingegneria, Società e Impresa, Università degli Studi della Tuscia, 01100 Viterbo, Italy; pelosi@unitus.it
- ³ Istituto di Chimica dei Composti Organometallici, Consiglio Nazionale delle Ricerche, 56124 Pisa, Italy; vincenzo.palleschi@cnr.it
- ⁴ Dipartimento di Scienze della Terra, Università degli Studi di Torino, 10125 Turin, Italy; francesca.lozar@unito.it (F.L.); cesare.comina@unito.it (C.C.); daniele.castelli@unito.it (D.C.)
- ⁵ Dipartimento Collezione e Ricerca, Museo Egizio, 10123 Turin, Italy; federico.poole@museoegizio.it
- ⁶ Freelance Conservator, 10100 Turin, Italy; alessia.spoladore@gmail.com
- * Correspondence: stefano.legnaioli@cnr.it; Tel.: +39-050-315222



Citation: Cavaleri, T.; Legnaioli, S.; Lozar, F.; Comina, C.; Poole, F.; Pelosi, C.; Spoladore, A.; Castelli, D.; Palleschi, V. A Multi-Analytical Study of an Ancient Egyptian Limestone Stele for Knowledge and Conservation Purposes: Recovering Hieroglyphs and Figurative Details by Image Analysis. *Heritage* **2021**, *4*, 1193–1207. <https://doi.org/10.3390/heritage4030066>

Academic Editor: Silvano Mignardi

Received: 19 June 2021

Accepted: 7 July 2021

Published: 12 July 2021

Publisher's Note: MDPI stays neutral with regard to jurisdictional claims in published maps and institutional affiliations.



Copyright: © 2021 by the authors. Licensee MDPI, Basel, Switzerland. This article is an open access article distributed under the terms and conditions of the Creative Commons Attribution (CC BY) license (<https://creativecommons.org/licenses/by/4.0/>).

Abstract: A multi-analytical study was carried out on an ancient Egyptian limestone stele with red figures and hieroglyphs (S. 6145) coming from the village of Deir el-Medina and belonging to the collection of the Museo Egizio (Turin, Italy). With the support of a multidisciplinary team, a project for the preservation and conservation of this stele provided an opportunity to carry out a very detailed study of the object. Petrographic and mineralogical analysis led to the characterization and dating of the limestone, and ultrasonic tests were of great help in shedding light on the state of preservation of the stele, as a preliminary to planning conservation treatment. The chemical nature of the red pigment was investigated by non-invasive spectroscopic analyses. Multispectral imaging and statistical image processing improved the readability of the hieroglyphs, whose preservation ranged from heavily compromised to almost completely invisible, revealing some signs that had previously not been visible.

Keywords: multispectral imaging (MSI); statistical image processing; recovering hieroglyphs; non-invasive spectroscopy; petrographical; mineralogical and micropaleontological analyses; ultrasonic measurements; limestone; ancient Egypt; commemorative stele; conservation

1. Introduction

The Museo Egizio in Turin, Italy, houses one of the most important collections of ancient Egyptian antiquities in the world. Its two main sources are the Drovetti collection, purchased in 1824, and artifacts from a number of excavations conducted in Egypt by the director of the museum, Ernesto Schiaparelli, between 1903 and 1920, and by his successor, Giulio Farina, in the 1930s. Interdisciplinary investigations of this collection relying on collaborations with research and conservation institutions are at the forefront of the Museo Egizio's current engagements.

The museum holds a limestone stele (S. 6145, Figure 1) of which only the upper part is preserved. It comes from the village of Deir el-Medina. This site is located in Upper Egypt in a valley behind the hill of Qurnet Murrai, on the left bank of the Nile, south-west of Sheikh-abd el-Qurna, facing the city of Thebes.

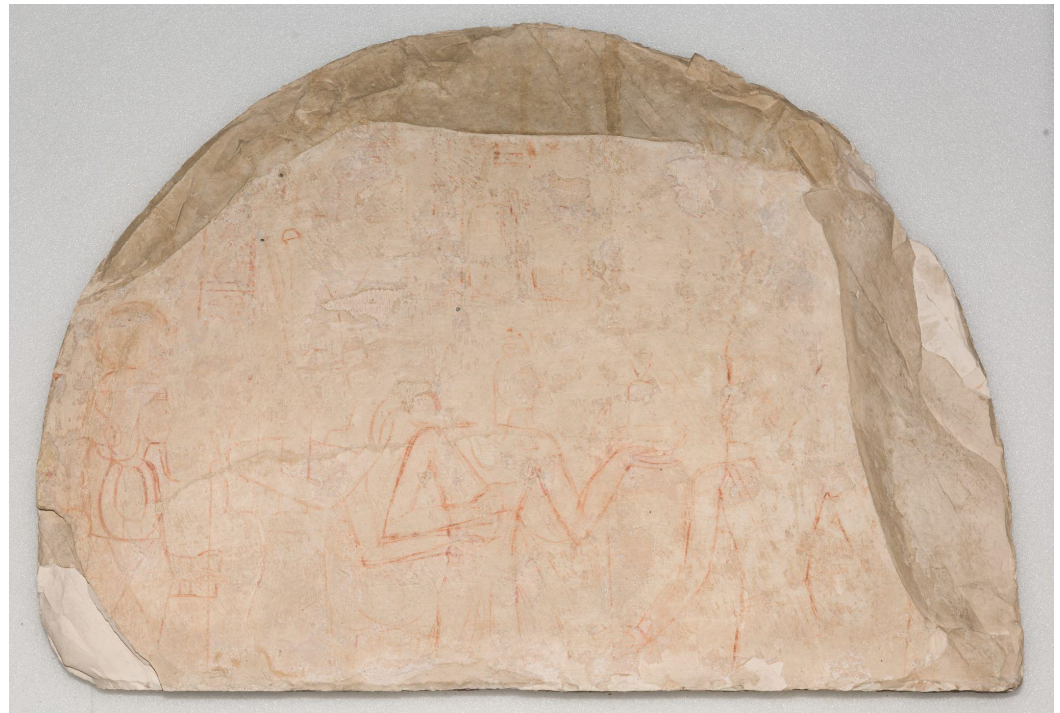


Figure 1. Stele from the village of Deir el-Medina. Turin, Museo Egizio, S. 6145. Photograph taken after the conservation treatment.

The village of Deir el-Medina was active throughout the New Kingdom (from the Eighteenth to the Twentieth Dynasty, 1539–1076 BC). It housed the workers employed to build the tombs in the Valley of the Kings and the Valley of the Queens. The stele was discovered during the 1905 campaign of the Italian Mission led by Ernesto Schiaparelli at Deir el-Medina, and was brought to the Museo Egizio in Turin in the framework of the sharing system (*“partage”*) regulating foreign excavations in Egypt at the time. Its provenance has been repeatedly stated to be chapel D in the sanctuary of Meretseger, south of the village along the path between Deir el-Medina and the Valley of the Queens [1,2]. However, the stele’s “high” inventory number suggests, on the contrary, that it does not belong to the lot of objects excavated here by the Italian Mission, which only encompass nos. S. 5987–6067 [3]. A provenance from the excavations conducted north of the village, in the area of the Ptolemaic temple, seems more likely [4].

Given its place of discovery and its content, the stele S. 6145 can be regarded as a commemorative stele. Stelae are most often found in tombs, where they evoked the main rite that ensured the connection between the deceased and the world of the living, namely, the bringing by the latter of the offerings that would allow the deceased’s survival in the afterlife. Other stelae, like this one, were instead made for votive purposes, to honour the gods. Their typological features are not different from those of funeral stelae, but their location and function are different: they are found inside temples or shrines, rather than in tombs, and are dedicated to the main deities of these places of worship.

As for the representation, the numerous traces of red hieroglyphs and figures present in the upper and underlying register of the stele appear to be faded and almost illegible. Because of its state of preservation, the documentary value of the stele, already partially compromised by the difficulty of reading especially the upper register, was exposed to further risk by a horizontal crack, which threatened to cause the detachment of a large fragment decorated with hieroglyphs. A similar loss of material had already affected much of the upper arched profile in the past.

This article starts from the multi-analytical study—material, technical, and Egyptological—conducted with the aim of preserving and investigating this object by a multidisciplinary team from the University of Turin (UniTo), the Museo Egizio in Turin, and the Fondazione

Centro per la Conservazione e il Restauro dei Beni Culturali La Venaria Reale (CCR), with the collaboration of the Institute of Chemistry of Organometallic Compounds of the Italian National Research Council (ICCOM-CNR) in Pisa [5]. In this study, a conservation treatment aimed at guaranteeing the transmission to others of the contents of a cultural document called for appropriate diagnostic investigations to guide the consolidation treatment and to allow the handling and cleaning of the artifact.

Specifically, we needed to investigate the constituent material to verify its intrinsic characteristics and assess the level of risk that cracking posed to the physical integrity of the artifact. Close observation to reveal the execution technique of the stele, the signs of working of the stone, and the original grouts served as a guide for the following microscope investigations on micro-samples of stone and grouting that underwent petrographical, mineralogical, and micropaleontological analyses [6].

The study of the crack required the stele to be analysed with ultrasonic-based techniques. When working on cultural heritage, tests and analyses of the integrity of a medium must be carried out with non-destructive techniques. Ultrasonic investigations are therefore among the most frequently adopted to evaluate deterioration and detect areas of structural weakness [5,7]. The method is based on the analysis of the apparent propagation velocity of an ultrasonic impulse within the medium. This velocity is obtained from the ratio between the distance of the travel path (the straight distance between the transmitting and the receiving probes) and the travel time measured by the instrumentation. The presence of altered material along the travel path results in a decrease in the apparent propagation velocity of the ultrasonic impulses. Analysing the ultrasonic propagation on a dense pattern of paths can therefore highlight the distribution of the velocities and consequently detect altered portions within the body, which, in this case, was fundamental for knowing the state of preservation of the stele.

Furthermore, we carried out a detailed surface study to spot traces of drawings no longer visible to the naked eye, but possibly by other means, in order to prevent the risk of removing them during cleaning. This required the use of spectroscopic analysis, for investigating the nature of the red pigment, and of multiband imaging and statistical image processing, for improving the readability of the hieroglyphs.

2. Materials and Methods

2.1. Materials

The object of this study and analysis was the limestone stele S. 6145 (see Figure 1), a large fragment of wall decoration measuring approximately $100 \times 100 \times 15 \text{ cm}^3$ coming from Deir el-Medina and belonging to the Museo Egizio collections. The stele shows numerous traces of red figures and hieroglyphs that appear to be faded and almost illegible, a preparatory drawing for carving in relief. At close observation the lower side of the artifact appeared to be crossed horizontally by a long crack, following the sedimentary stratification of the stone. This crack intersected the figures and threatened their preservation.

In addition, four samples were studied and analysed. Two of them (samples 1 and 3) were not taken from the stele, being previously detached fragments received with the object. One of them (sample 2) was taken from the reverse of the stele, whereas one (sample 4) came from an original grouting on the front of the stele.

2.2. Experimental Study and Methods

The first step of the experimental study was focused on investigating the nature and state of preservation of the support and the related aspects of technique of execution (signs of working, original grouts). This step was carried out with a multi-technical approach using scanning electron microscopy energy dispersive x-ray spectroscopy (SEM-EDS) and x-ray diffraction (XRD) analyses on samples and with non-invasive ultrasonic measurements on the stele; the latest aimed at better specifying the extent and entity of the fractured zone and verifying the presence of further discontinuities nonvisible to the naked eye.

Specifically, samples 1, 2, and 3 were investigated with petrographical, mineralogical, and micropaleontological analyses at the Department of Earth Sciences of the University of Turin. For SEM-EDS tests, the samples were mounted on stubs and analyzed with a JEOL JSM IT300LV (high vacuum—low vacuum 10/650 Pa—0.3–30 kV) scanning electron microscope equipped with an EDS Oxford INCA Energy 200 microanalysis and an INCA X-act SDD thin window detector. For a micropaleontological investigation of the calcareous nanofossil content, smear slides were prepared with the standard technique [8] and observed at 1250 \times in transmitted light with a B50X Olympus polarized microscope.

Sample 4 was analysed by XRD. The analysis was carried out with a Rigaku Miniflex II with a high frequency x-ray tube with a copper anode, powered by a 30 kV and 15 mA fixed current. The vertical goniometer had a radius of 150 mm and a 2 θ measuring range between -3° and 145° . The detector was a NaI (Ti) scintillator counter, which was 23 mm in diameter. The spectra acquisition was made with the MDI Jade 9.0 software.

Ultrasonic measurements were executed on the stele with a dense grid of measuring points. To perform the ultrasonic analysis, an ultrasonic pulse generation instrument (Pundit-Proceq) with exponential transmitting and receiving probes, with a nominal frequency of 50 kHz, was employed. The instrument was connected to a notebook with appropriate software for storing and analysing the measured data. The measurements were executed on the surface of the stele along a grid of 147 measuring points spaced approximately 5 cm apart. The grid (red dots in Figure 2) was laid out by superimposing a sheet of melinex onto the stele. Measurements were conducted both in the horizontal and vertical directions among each couple of measuring points for a total of 268 measurements. Both the transmitting and receiving probes were placed in contact with the melinex paper at an angle of about 45° to the surface of the stele, to allow penetration of the ultrasonic pulse within the material. The ultrasonic pulse travel times were obtained for each measurement by manual picking of first arrivals on the received traces. All the acquired velocity values were then merged and interpolated in the Surfer software to allow for the reconstruction of the velocity field of the stele.

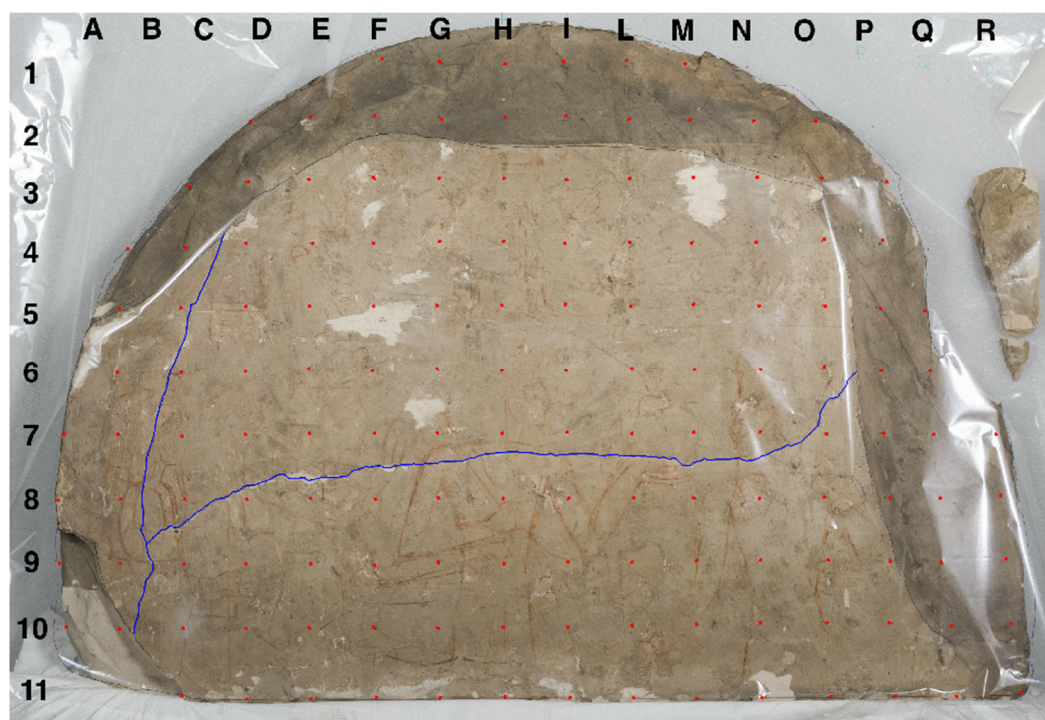


Figure 2. The image shows the dot pattern employed to carry out the ultrasonic test.

The second step of the experimental study was aimed at recovering the legibility of the hieroglyphs and red figures. For this step, a totally non-invasive multi-analytical

approach was adopted, which was followed by the Egyptological analysis, also intended as validation of the technique.

Preliminary investigation was first conducted through close observation and multi-band imaging techniques commonly applied to cultural heritage, specifically, visible fluorescence induced by UV radiation (UVF) and IR photography. The UVF images were acquired with a Nikon D810 full-frame reflex camera mounting a PECA 916 filter, irradiating the artifact with UV Labino[®] lamps (365 nm-emission peak). The IR photographs were acquired with a Nikon D810 IRUV full-frame reflex camera mounting a B + W 093 filter, illuminated with Ianiro Varibeam Halogen 800 W lamps. The acquisition required the use of a 24-colour XRITE Classic ColorChecker[®] and a 99% reflective white ceramic tab as references. The images were colour-corrected and white-balanced in post-production in Adobe Lightroom.

As for the spectroscopic analyses to confirm the chemical nature of the red colour, which were already hypothesized on the basis of the literature and multiband imaging outcomes, some points of the drawings on the stele were examined by x-ray fluorescence (XRF) and fiber optics reflectance spectroscopy (FORS). The XRF analyses were carried out with a Bruker Tracer III-SD handheld XRF spectrometer, which had an x-ray tube with a Radium (Rh) anode. The measurements were made at 40 kV, 10 μ A, and 60 s acquisition time. FORS spectra were acquired in the 350–1000 nm range with a spectral resolution of about 0.5 nm by using an Ocean Optics HR2000 + ES spectrophotometer, an Ocean Optics HL2000 halogen lamp, optical fibres of 400 μ m in diameter, and a Spectralon $\text{\textcircled{C}}$ 99% white reference. The analyses were carried out in a $2 \times 45^\circ/0^\circ$ geometry following the CIE standard illuminating/viewing geometry [9] on a measuring area of fixed dimensions (approximately 3 mm in diameter).

To improve the readability of the hieroglyphs, the MultiSpectral Imaging technique (MSI) was applied to the stele. For the MSI analysis, we used a system equipped with a high-resolution Moravian G2-8300 camera (CCD detector KAF-8300, imaging area 18.1×13.7 mm, pixel size 5.4×5.4 μ m) with a high dynamic range (16 bits). The sensor was cooled to reduce the electronic noise during the acquisition. The spectral resolution was obtained through the use of interferentials (± 25 nm band pass around the central wavelengths) at 400, 450, 500, 550, 600, and 650, in the visible range, and 850, 950, and 1050 nm in the near infrared. Two sets of nine acquisitions were carried out for the different available bands (Table 1), one of them using visible light as an illuminator and the second one with UV LEDs (10 V). In the first case, the integration time was set to 1 s for acquisitions from 550 to 950 nm and increased up to 10 s for those from 400 to 500 nm and to 15 s for the 1050 nm band, maintaining the same lighting condition for the visible and infrared image sequence.

Table 1. Experimental parameters of the MSI acquisition.

Spectral Band (nm)	Vis Acquisition Time (s)	UV Acquisition Time (s)	Aperture
400	10	15	11
450	10	15	11
500	10	30	11
550	1	30	11
600	1	45	11
650	1	90	11
850	1	90	11
950	1	120	11
1050	15	400	11

After the images have been acquired, they must be registered to compensate the unavoidable shifts and distortions introduced by the different filters interposed between the objective and the sensor of the CCD camera. To this purpose, a specialized software made by the Institute of Science and Technologies of Information of the CNR was used [10], which

guarantees sub-pixel accuracy in image recording. The colour image was reconstructed through the superposition of three images acquired sequentially in the fundamental RGB spectral bands (450–550–650), and similarly for the false IR colour (550–650–1050). Then, statistical separation was applied to the whole set of 18 multispectral images.

3. Results

3.1. Characterization, Provenance, and Stratigraphical Age of the Limestone Support

The stele S. 6145 was made out of a clayey limestone (sedimentary rock), which was pale beige in colour. It had a very fine-grained, homegranular, massive structure without evident stratification. The fracture was typically conchoidal. Small bodies, with a subspherical to ovoid shape, dark grey in colour, occurred on the surface of the stele (Figure 3). Two were located on the front and two on the reverse of the stele, and they were characterized by a blackish border. They varied from a few mm to 2–3 cm in size. Their fine grain size is not distinguishable to the naked eye, and the exposed surfaces showed a typical conchoidal fracture. All these characteristics are typical of chert nodules, which are common features of calcareous sedimentary rocks.



Figure 3. Chert nodules, millimetric in size, on the front of the stele (a,b). Chert nodules, centimetric in size, on the reverse of the stele (c,d); the second one contains two smaller nodules (d).

On the reverse of the stele, well-closed microfracture systems can be identified (Figure 4). These are clearly visible on the surface but are less visible transversely. Their spacing is pluricentimetric, with their lateral extension up to decimetric, extending over much of the stele. These fractures could be either syn-sedimentary or tectonic in origin.

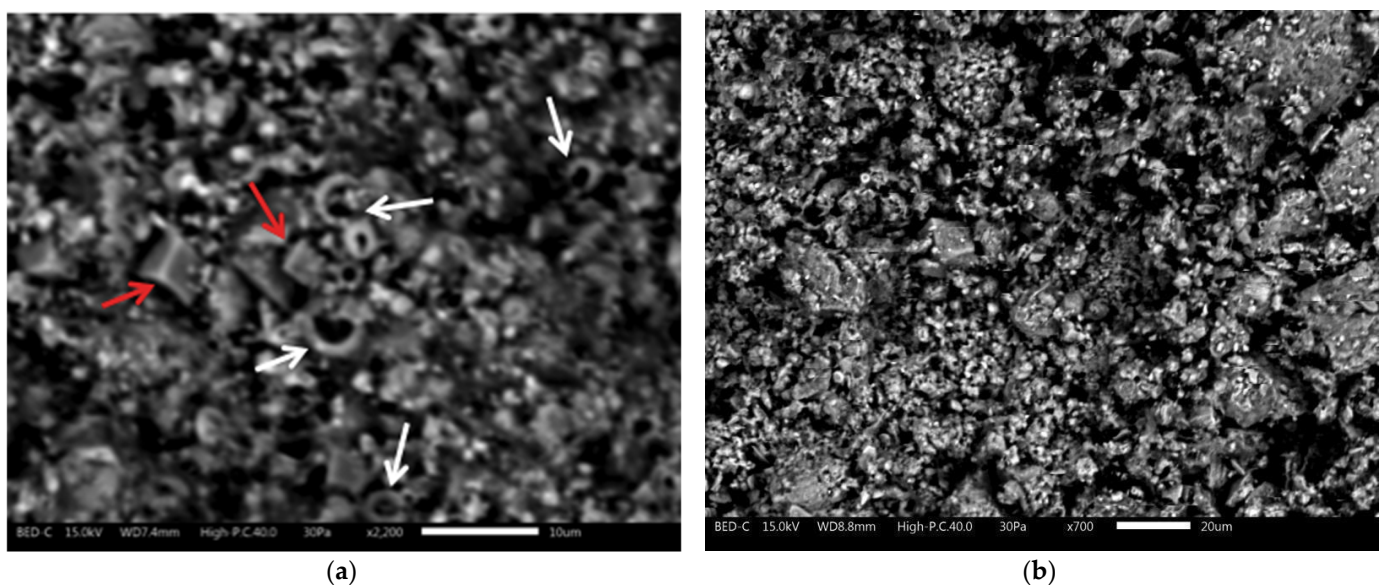
During the processing of the reverse, these systems influenced the development and extension of fracture surfaces in a typically conchoidal pattern.

The limestone support, studied in smear slides under the optical microscope, showed abundant micrite together with minor micrometric dolomite crystals, probably diagenetic in origin, as is also suggested by the moderate to poor preservation of the microfossil remains. No traces of pyrite or glauconite were found, although they have been reported in some Egyptian lithotypes.



Figure 4. Closed, subparallel microfracture systems, with centimetric spacing, visible on the reverse of the stele.

SEM-EDS investigations on samples allowed us to better detail the petrographic and micropaleontological features of the limestone. Sample 1 (not taken from the stele but a previously detached fragment) confirmed the carbonatic nature of the rock, its fine grain size (a few microns; Figure 5a), and the presence of micrometric crystals of dolomite; the micropaleontological content, consisting of coccoliths, was also clearly visible. These observations confirmed that the rock formed from the lithification of a carbonate sediment deposited in a marine environment, possibly at depths greater than the photic zone. Sample 2 (taken from the reverse of the stele) shows areas where the original surface of the rock (micrite) can be observed and areas where a mixed coating was observed, which was also composed of quartz grains (Figure 5b).



(a)

(b)

Figure 5. Electron microscope image (SEM backscattered electrons) of: (a) sample 1; the fine grain size of the micrite crystals is clearly visible; white arrows: micropaleontological content (coccoliths); red arrows: dolomite crystals; (b) sample 2, microscopic aspect: micritic crystals and euhedral crystals.

The calcareous nannofossil assemblage is well diversified and dominated by *Ericsonia formosa*, *Chiasmolithus nitidus*, *Toweius pertusus*, *Coccolithus pelagicus*, *C. crassus*; small *Toweius* specimens were also present but unidentifiable at the species level. Rare *Sphaerolithus moriformis*, *S. radians*, *Biantholithus flosculosus*, *Cyclicargolithus luminis*, and *C. pauxillus* complete the semisedentary assemblage. The sample also contained rare *Neocrepidolithus fossus*, *Ericsonia aliquanta*, and *Fasciculithus tympaniformis*, likely re-worked from older sediments (Palaeocene in age).

On the basis of this assemblage, and of the absence of *Tribrachiathus orthostylus*, a species that characterizes the homonymous biozone [11], and of *Discoaster sublodoensis* (marker of the CNE6 biozone), it is possible to assign the sample to the CNE5 biozone, with a Ypresian age (lower Eocene). This is also supported by the presence of *C. crassus*, which appears at the top of the CNE4 biozone [11]. As for the standard biozones, still in use by many authors, the sample belongs to the biozones CP11 [12] and NP13 [13], thus confirming a Ypresian age. This age assignment and its lithological characteristics allow us to attribute the sample to the Thebes Fm. Limestones with dolomite (and pyrite, which was absent in the sample) also occur at the base of the Esna Fm. According to some authors [14], the Esna Fm. dates from the Palaeocene, and, according to others, it dates to the Eocene age [15]; thus, in both cases it would be older than the studied sample. The stratigraphy of the Eocene limestones from central Egypt, cropping out around the area of Thebes and Luxor—where the global stratigraphic standard section and point (GSSP) of the Eocene [16] is located—and the stratigraphy of the necropolis of the pharaohs [15,17] suggest possible interpretations based on the data collected.

The presence of dolomite is known throughout the Thebes Fm. [17], particularly in lithological Units B4 and D1. However, the assemblage characterized by the absence of *T. orthostylus* is similar to that reported by King et al. (2017) in part of the section of Jebel Gurnah, starting from Units H and I. Up to Unit E, the limestone contains planktonic foraminifera with a decreasing upward abundance, indicating a shallowing upward trend, which culminates with the overlying shallow water nummulitic limestones, devoid of planktonic foraminifera. The authors also report that the limestones of Units B4 and D1 may contain nummulites. All other limestones of the lithological units of the Thebes Fm. are bioclastic and/or nodular, or marly-clayey and therefore cannot be correlated with the stratigraphic level of origin of the stele.

It thus seems reasonable to attribute the sample, which belongs to the Biozone CNE5 (=CP11 and CN13), to a level that can be correlated with Unit H of the Thebes Fm. of the section of Jebel Gurnah, in agreement with the findings of King et al. (2017).

Finally, sample 3 (not taken from the stele, but a previously detached fragment) showed a completely different appearance, consisting of an aggregate of elongated acicular crystals of plurimicrometric size (often larger than 10 microns) and rare larger tabular crystals. The EDS analyses showed that these are gypsum crystals; the sample could therefore come from the original grouting of the stele, as confirmed by the XRD analyses (see after).

3.2. Technique of Execution and State of Preservation of the Support

Stele S. 6145 has three different levels of processing. The back is roughly hewn to make it approximately flat. The sides are more finely cut but not finished. The front, being meant to accommodate the decoration, has a flat surface, smoothed and locally grouted, probably to remedy constitutive imperfections or accidental ones produced during the manufacturing process. The pale beige surface of the stele shows several such grouts of whitish colour. They appear compact and can be traced back to the original Egyptian manufacture of the object, since the preparatory drawing intersects them. Thanks to the UVF imaging, all the grouts present on the stele were observed, including some not visible to the naked eye (Figure 6). XRD analysis allowed us to identify their composition, detecting the presence of anhydrite, calcite, quartz, dolomite, and gypsum (sample 4, taken from the stele in correspondence to an original grout).

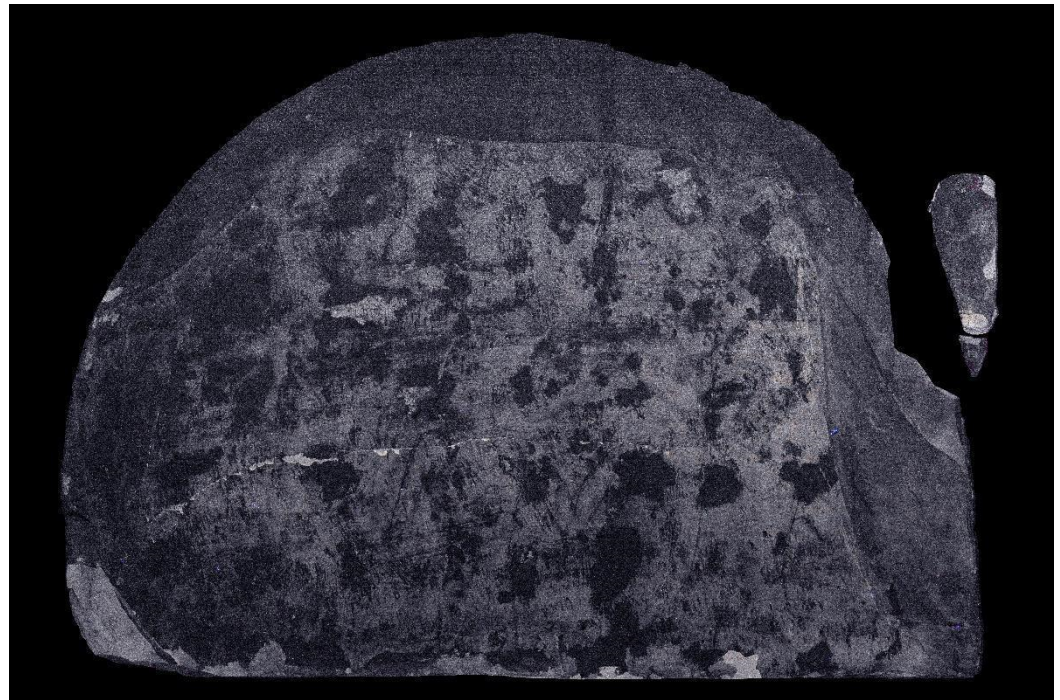


Figure 6. UV fluorescence image of the stele (UVF).

In addition to the closed microfractures described above, the stone material constituting the stele has a crack extending across the entire width of the stele. Its development and direction were influenced by the sedimentary structure of the limestone. By observing the object from the side, one can indeed see that the fracture is substantially parallel to sub-parallel to the barely visible stratification of the limestone (Figure 7).



Figure 7. Lateral picture of the stele, showing (in blue) the direction of the crack, which is subparallel to the sedimentation.

The ultrasonic test yielded medium-high velocity values (approximately around 2200 m/s) for most of the stele but also evidenced a localized reduction in the velocity (to about 1000 m/s). The velocity distribution along the stele evidenced a very good correspondence of the low-velocity area (blue–purple area in Figure 8) with the known location of the main visible fractures on the surface of the stele (see Figure 2). No other specific low-velocity zones were observed. The relevance of this low-velocity area and its particularly low-velocity range allowed us to establish a significant persistence of the fractured zone, which can be regarded as a warning of the existence of a threat to the integrity of the stele, particularly during handling.

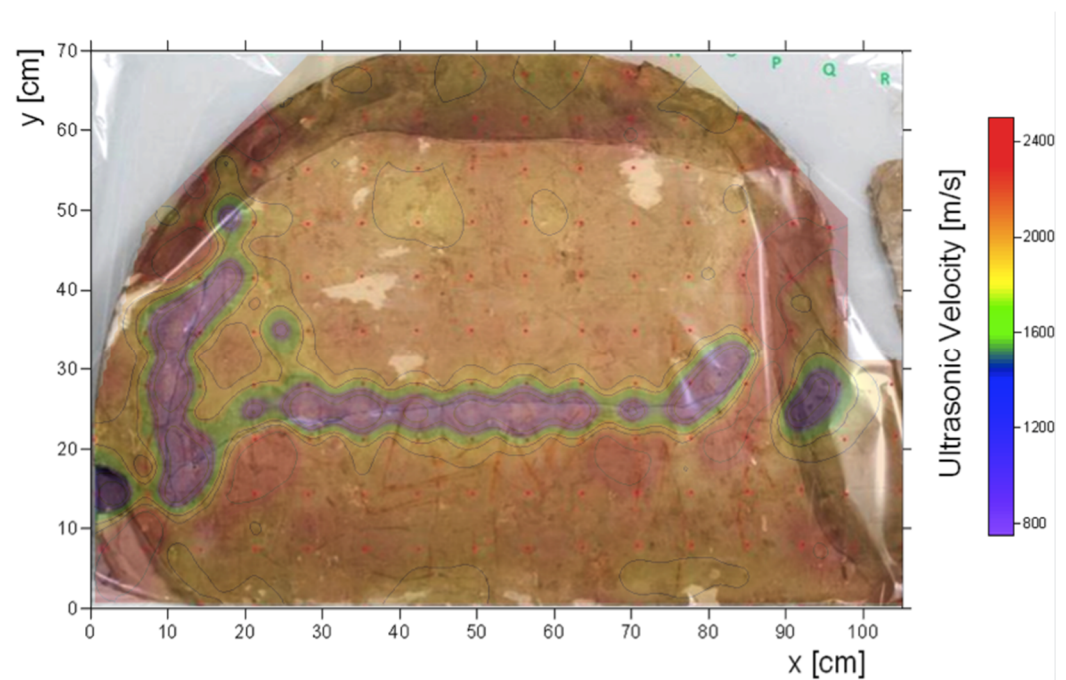


Figure 8. Ultrasonic velocity distribution along the stele.

3.3. The Decoration: Recovering the Figures and Their Accompanying Hieroglyphic Inscriptions

The decoration of the stele consists of a preparatory drawing for the carving of a figured scene with hieroglyphic captions in its upper part (the lunette). Based on the literature and the analyses, the figures and inscriptions are presumably drawn in red ochre. In ancient times, the red earth was extracted from deposits in Upper Egypt in the Abu Simbel area, along the coastal strip of the Red Sea and in the Sinai Peninsula. Vitruvius and Dioscorides mention that Egypt yielded the best red ochres. The XRF analysis indeed detected the presence of iron, with lower signals of silicon and titanium, as well as calcium, strontium, and a feeble sulphur signal attributable to the support. The red colour, applied directly on the limestone, presumably had a gum arabic binder, as widely reported in the literature [18].

As expected, neither the UVF nor the IR photographs have been of great use for improving the readability of the hieroglyphs, since red ochre in a gum arabic binder does not have a strong absorption in the photographic infrared region nor a particularly intense fluorescence when illuminated with 365 nm UV radiation.

Figure 9 shows the three RGB acquisitions and the most significant channel in the near infrared at 1050 nm of the upper part of the stele.

Whereas the raw images acquired with the MSI did not improve readability, the BSS algorithm greatly improved it. Figure 10 reports the most significant BSS result: it is worth noting that the picture is the composition of different images that were acquired to cover the whole upper surface of the stele.

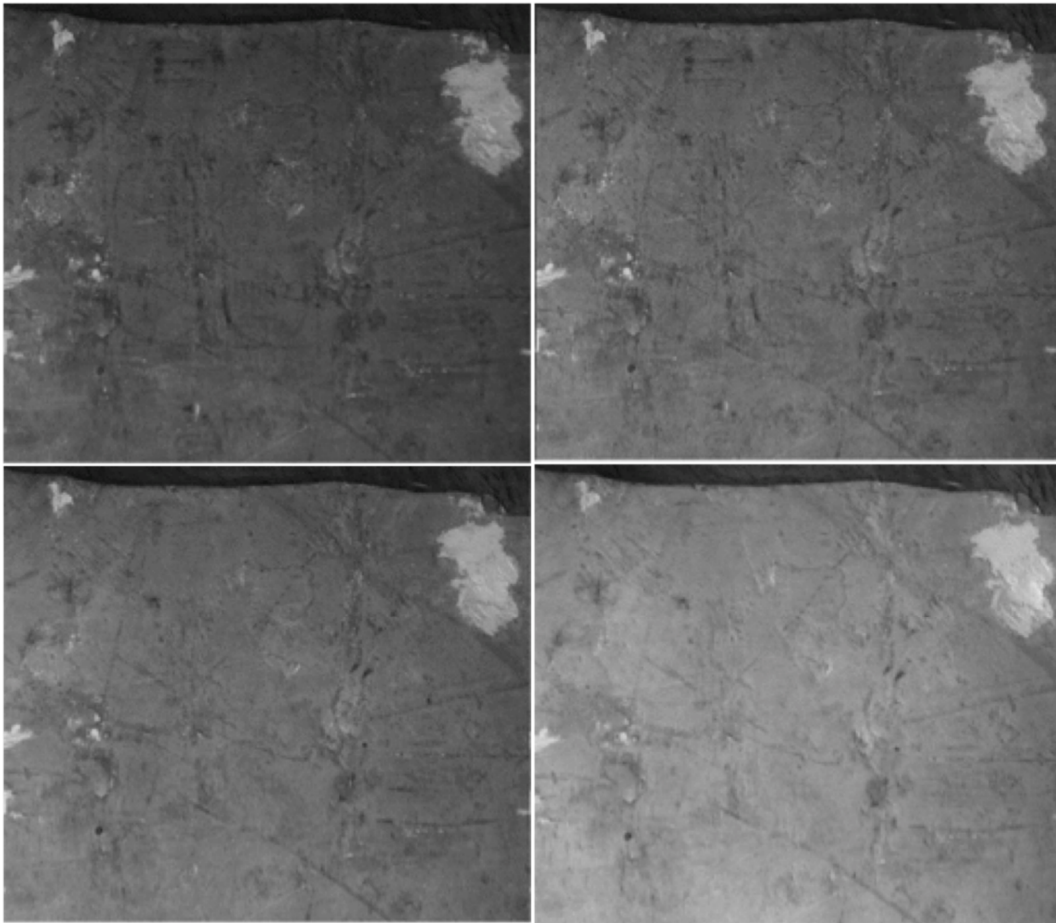


Figure 9. MSI of a detail of the stele: images taken at 450, 550, 650, and 1050 nm.

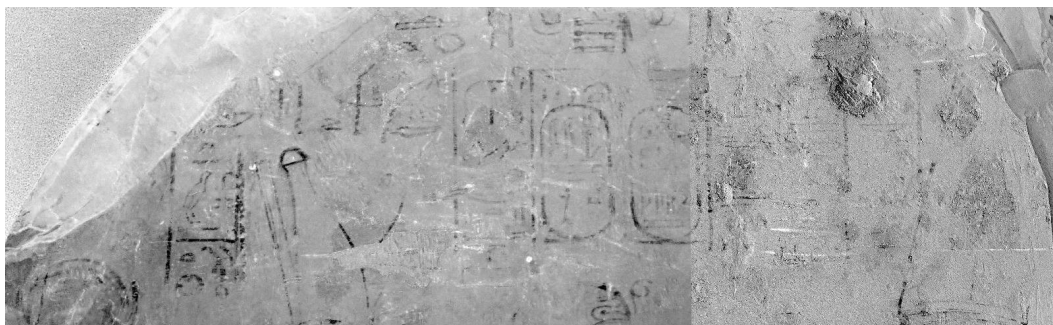


Figure 10. Output of the BSS algorithm used for enhancing the readability of the hieroglyphic text in the stele S. 6145.

As described below, a different form of image processing based on the chromatic derivative imaging (ChromaDI) method allowed recovery of the readability of the stele (Figure 11). This method, developed by Pisa groups [19,20], exploits the subtraction of consecutive couples of four consecutive spectral images, namely, G-B, R-G, and IR-R.

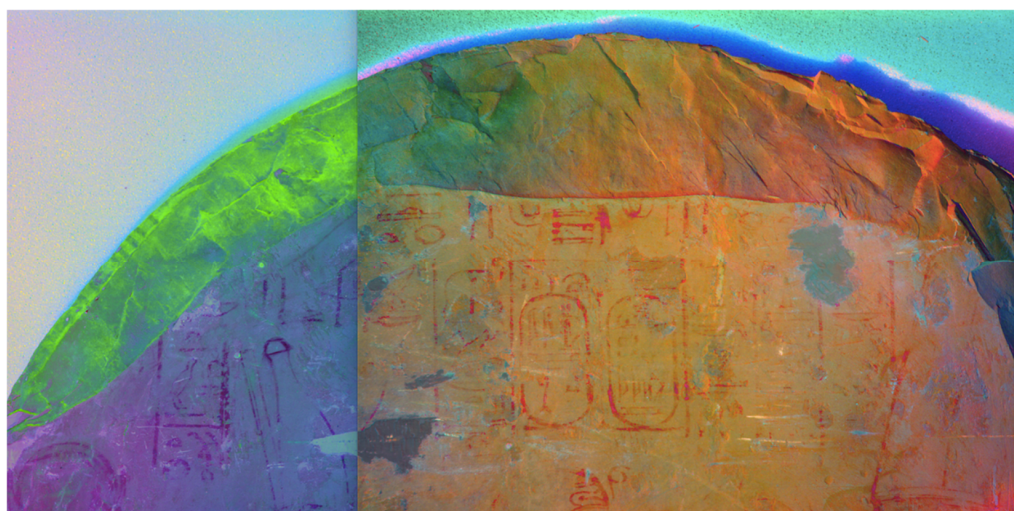


Figure 11. ChromaD images corresponding to the four multispectral series considered. The picture is the composition of different images that were acquired to cover the whole upper surface of the stele.

At the top of the stele the lower coil of two cobras (uraei) can be made out, what is left of the usual motif of the sun disk with uraei topping the lunette of such stelae. On either side, the hieroglyphs for “the great god, the Behdetite” can be made out. The text between the uraei appears to read “beloved of Amun.” The main scene shows the pharaoh Seti II (1202–1198 BCE), in the middle, his left hand held up to receive the symbol of the royal jubilee, the *heb sed*, which hangs from a palm shoot (the hieroglyph for “year”) held forth by the god Amun with his left hand. Seti is bearded and clad in a kilt and holds the *heka* scepter in his right hand. On his head he wears the royal headcloth (*nemes*) topped by the cobra (uraeus). Amun, also kilted, wears his usual two-feathered crown and holds the *was* scepter in his right hand. A profile line descending obliquely behind the figure of Amun may belong to a figure of another deity, identified as Ptah in the literature [1,2] (pp. 125–126). Behind the king are the two other members of the Theban divine triad, with their usual attributes: the goddess Mut, wearing a dress and the Double Crown, and the child-god Khonsu, mummiform and bearded, wearing the sidelock of childhood, the lunar disk on his head, and a necklace, and holding the *was* sceptre. Most of the signs in the inscription above Amun appear to be faded beyond recognition, even in the processed images; we can make out the cobra-glyph at the very beginning of the inscription (arranged in columns, going from left to right)—which is the first sign of the group *djed medu* (“Saying the words”)—and the sign for *.k*, “you” (in what could be the expression *di.en.i ene.k*, “I have given you . . .”, referring to the god’s granting of the jubilee to the king), as well as the throne glyph in “(lord of the) thrones (of the Two Lands).” Above the king are his two royal names (prenomen, nomen), which are entirely readable in the multispectral images: “The lord of the Two Lands (Weser)-khepru-Re-mery-Amun, the lord of apparitions Setymery-en-Ptah.” Above Mut we read, from right to left: “Saying the words by Mut, mistress of the sky: ‘I am your mother . . .’” Above Khonsu is what looks like a basket (a *neb-* or *k*-sign) followed by “Khonsu in Thebes.”

The stele was published about fifty years ago in the volume of the Museo Egizio’s general catalogue devoted to the stelae of Deir el-Medina [2] (pp. 125–126, 301, with further literature). The images were correctly identified and what was visible of their captions read. MSI imaging, however, has enabled us to improve on these authors’ naked-eye readings, revealing signs that were not visible to them, notably:

- The *weser* (head and neck of canine animal) and *kheper* (scarab) sign in the prenominal of the king, Weser-khepru-Re (correctly reconstructed by Tosi and Roccati, but not actually seen).
- The independent pronoun *inek* (“I (am)”: a jar above a shallow basket with a handle, read as *k*) beginning the goddess Mut’s utterance.

- The cobra sign (*dj*) at the beginning of the text above Amun.
- The *k* pronoun (the shallow basket with a handle) in the text above Amun.

The MSI imaging also allowed the details of the figures of the king and the gods to be distinguished more clearly.

Finally, Figure 12 shows the picture obtained by overlapping the RGB image with the pattern obtained with the most significant BSS output. This method enables a sort of “virtual restoration” of the original heritage object, useful for its study and for making it more fully understandable to scholars and the general public.

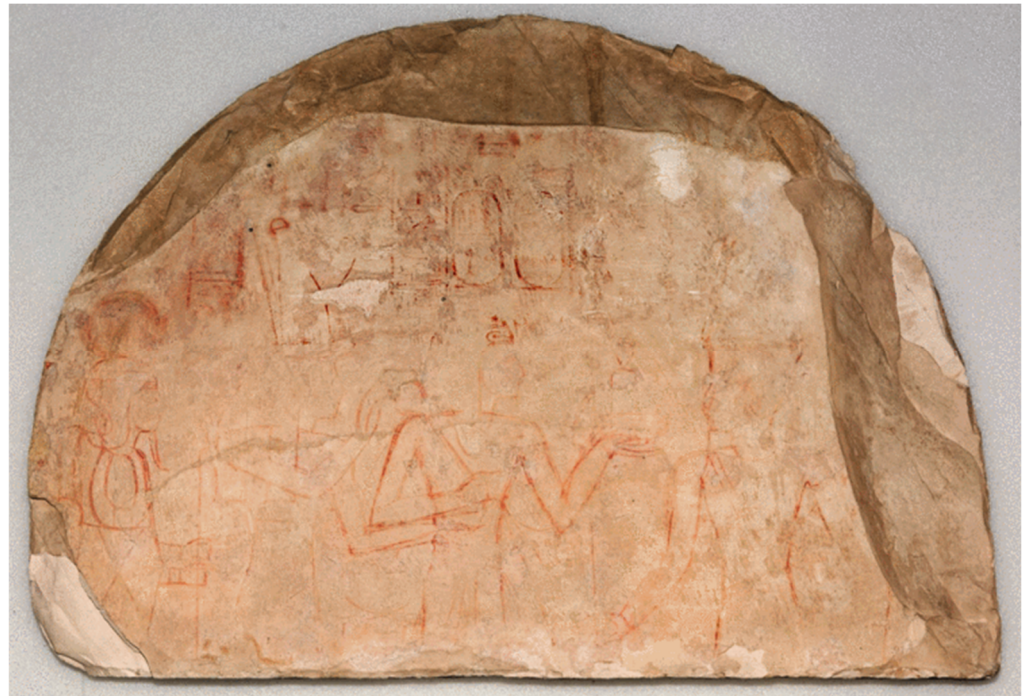


Figure 12. RGB image overlapped with the pattern obtained with the most significant BSS output (virtual restoration).

4. Discussion

The material, technical, and Egyptological study conducted on the stele S. 6145 led to a deep knowledge of the object that allowed us to plan the preservation and conservation treatment. The micropaleontological, mineralogical, and petrographical analyses confirmed that the lithic support of the stele consists of micritic limestone with minor dolomite crystals and chert, containing calcareous nannofossils (but devoid of planktonic foraminifera), allowing an assignment to the CNE5 biozone (Ypresian age; lower Eocene). The lithological and micropaleontological characteristics confirm the stele’s provenance from the Thebes Fm.

As for the long crack crossing the limestone support horizontally, the identification of the internal discontinuity through ultrasonic analyses inevitably imposed a reflection on possible conservation choices and on the present and future precautions to be adopted in handling the artifact. For example, it was turned over on its back only after being placed inside its crate. These analyses were crucial in anticipation of the transportation of the stele and its possible future museum exhibition.

Close observation revealed the execution technique of the stele, first of all recognizing the signs of working of the stone and the original grouts, whose composition was analysed by combining XRD and SEM-EDS as complementary techniques. Non-invasive spectroscopic analyses allowed confirmation of the executive technique and chemical nature of the red pigment. It deals with a preparatory drawing for carving in relief: in fact, the red ochre is spread directly on the support, without any preparation layer.

We demonstrated the advantages of using MSI and BSS algorithms to enhance hidden patterns in archaeological stelae, using an approach so far limited to paintings and ancient manuscripts. The multispectral investigation made it possible to see and read several hieroglyphs that had not been distinguished by previous scholars. Furthermore, the resulting published images offer much more detail to readers than a natural-light photograph would. Depending on the spectral response of the materials and their conservation state, sometimes satisfactory results can be obtained even when limiting the analysis only to one of the infrared bands; more often, however, more sophisticated tests are called for, like those reported upon in this article.

Author Contributions: Conceptualization, T.C. and S.L.; data curation, T.C., S.L., F.L., C.C., D.C., and V.P.; formal analysis, T.C., S.L., F.P., and D.C.; investigation, T.C., S.L., F.L., C.C., F.P., D.C., and V.P.; methodology, T.C., S.L., F.L., and V.P.; project administration, T.C.; resources, F.P. and A.S.; supervision, T.C., C.P., and V.P.; validation, F.P.; visualization, F.L., C.C., A.S., and D.C.; writing—original draft, T.C., S.L., F.L., F.P., and A.S.; writing—review & editing, T.C., S.L., F.L., C.C., F.P., C.P., and D.C. All authors have read and agreed to the published version of the manuscript.

Funding: This research received no external funding.

Acknowledgments: We warmly thank the Museo Egizio, Turin and the Soprintendenza Archeologica, Belle Arti e Paesaggio per la Città Metropolitana di Torino for making this study possible. We would also like to thank Francesco Brigadeci, University of Turin, who acted as conservator tutor in Alessia Spoladore's thesis and Paolo Gallo, University of Turin, for being part of the teacher team of the same thesis. The stele S. 6145 was in fact the subject of a thesis of the master's degree course in Conservazione e Restauro dei Beni Culturali, a training course with qualification in accordance with Leg. Dec. No. 42/2004 offered by the University of Turin through the Centro Conservazione e Restauro "La Venaria Reale." We also thank the Laboratorio Analisi Scientifiche of the Soprintendenza Regione Autonoma Valle d'Aosta for the XRD and XRF analyses. Finally, our gratitude goes to Paolo Del Vesco, Museo Egizio Turin, and Ikram Ghabriel for their archaeological insight.

Conflicts of Interest: The authors declare no conflict of interest.

References

1. Bruyère, B. Mert Seger à Deir el Médineh. In *Mémoire Publiées par les Membres de L'institut Français D'archéologie Orientale du Caire*, 1st ed.; IFAO: Le Caire, Egypt, 1929–1930; Volume 1–2.
2. Tosi, M.; Roccati, A. Stele e altre epigrafi di Deir el Medina. N. 50001-50262. In *Catalogo del Museo Egizio di Torino*; Serie Seconda, Collezioni 1; Edizioni d'Arte Fratelli Pozzo: Torino, Italy, 1972.
3. Del Vesco, P.; Poole, F. Deir el-Medina in the Egyptian Museum of Turin. An Overview, and the Way Forward. In *Outside the Box: Selected Papers from the Conference "Deir el-Medina and the Theban Necropolis in Contact"*, Liège, Belgium, 27–29 October 2014; Dorn, A., Polis, S., Eds.; Presses Universitaires de Liège: Liège, Belgium, 2018.
4. Ghabriel, I. The So-Called Oratory of Ptah and Mertsger Re-Examined. In *Proceedings of the Deir el-Medina through the Kaleidoscope—2018 Turin International Workshop*, Modena and Torino, Italy, 8–10 October 2018.
5. Sambuelli, L.; Böhm, G.; Capizzi, P.; Cardarelli, E.; Cosentino, P. Comparison between GPR measurements and ultrasonic tomography with different inversion algorithms: An application to the base of an ancient Egyptian sculpture. *J. Geophys. Eng.* **2011**, *8*, S106–S116. [[CrossRef](#)]
6. Spoladore, A. The stele S.06145 from the village of Deir El-Medina and conserved in the Egyptian Museum of Turin: Handling, Reading and Conservation Problems. Master's Thesis, University of Turin, Venaria Reale, Italy, 25 November 2019.
7. Capizzi, P.; Cosentino, P.L.; Schiavone, S. Some tests of 3D ultrasonic travelttime tomography on the Eleonora d'Aragona statue (F. Laurana, 1468). *J. Appl. Geophys.* **2013**, *91*, 14–20. [[CrossRef](#)]
8. Bown, P.R.; Young, J.R. Techniques. In *Calcareous Nannofossil Biostratigraphy*. *British Micropalaeontological Society Series*; Bown, P.R., Ed.; Chapman and Hall: London, UK, 1998; pp. 1–15.
9. Oleari, C. *Misurare il Colore*; Hoepli: Florence, Italy, 2008; pp. 53–60.
10. Salerno, E.; Tonazzini, A.; Grifoni, E.; Lorenzetti, G.; Legnaioli, S.; Lezzerini, M.; Marras, L.; Palleschi, V. Analysis of multispectral images in cultural heritage and archaeology. *J. Appl. Laser Spectrosc.* **2014**, *1*, 22–27.
11. Agnini, C.; Monechi, S.; Raffi, I. Calcareous nannofossil biostratigraphy: Historical background and application in Cenozoic chronostratigraphy. *Lethaia* **2017**, *50*, 447–463. [[CrossRef](#)]
12. Okada, H.; Bukry, D. Supplementary modification and introduction of code numbers to the low-latitude coccolith biostratigraphic zonation (Bukry, 1973; 1975). *Mar. Micropaleontol.* **1980**, *5*, 321–325. [[CrossRef](#)]

13. Martini, E. Standard Tertiary and Quaternary calcareous nannoplankton zonation. In Proceedings of the II Planktonic Conference, Roma, 1970; Farinacci, A., Ed.; Edizioni Tecnoscienza: Rome, Italy, 1971; Volume 2, pp. 739–785.
14. Abu-Ali, R.; El-Kammar, A.; Zakaria, A.; El-Shafeiy, M.; Kuss, J. Paleo-environmental reconstructions of the Upper Cretaceous–Paleogene successions, Safaga, Egypt. *J. Afr. Earth Sci.* **2019**, *149*, 170–193. [[CrossRef](#)]
15. Aubry, M.P.; Berggren, W.A.; Dupuis, C.; Ghaly, H.; Ward, D.; King, C.; Knox, R.; Ouda, K.; Youssef, M.; Fathi Galal, W. Pharaonic necrostratigraphy: A review of geological and archaeological studies in the Theban Necropolis, Luxor, West Bank, Egypt. *Terra Nova* **2009**, *21*, 237–256. [[CrossRef](#)]
16. Aubry, M.-P.; Ouda, K.; Dupuis, C.; Berggren, W.A.; Van Couvering, J.A.; The Members of the Working Group on the Paleocene/Eocene Boundary. The Global Standard Stratotype-section and Point (GSSP) for the Eocene Series in the Dababiya section (Egypt). *Episodes* **2007**, *30*, 271–286. [[CrossRef](#)] [[PubMed](#)]
17. King, C.; Dupuis, C.; Aubry, M.P.; Berggren, W.A.; Knox, R.O.B.; Galal, W.-F.; Baele, J.-M. Anatomy of a mountain: The Thebes limestone formation (lower Eocene) at Gebel Gurnah, Luxor, Nile valley, upper Egypt. *J. Afr. Earth Sci.* **2017**, *136*, 61–108. [[CrossRef](#)]
18. Newman, R.; Serpico, M. Adhesive and Binders. In *Ancient Egyptian Materials and Technology*; Nicholson, P.T., Shaw, I., Eds.; Cambridge University Press: Cambridge, UK, 2000; pp. 475–493.
19. Legnaioli, S.; Grifoni, E.; Lorenzetti, G.; Marras, L.; Pardini, L.; Palleschi, V.; Salerno, E.; Tonazzini, A. Enhancement of hidden patterns in paintings using statistical analysis. *J. Cult. Herit.* **2013**, *14*, S66–S70. [[CrossRef](#)]
20. Legnaioli, S.; Lorenzetti, G.; Cavalcanti, G.H.; Grifoni, E.; Marras, L.; Tonazzini, A.; Salerno, E.; Pallecchi, P.; Giachi, G.; Palleschi, V. Recovery of archaeological wall paintings using novel multispectral imaging approaches. *Herit. Sci.* **2013**, *1*, 1–9. [[CrossRef](#)]